Distribution-free stochastic model updating of dynamic systems with parameter dependencies

Masaru Kitahara [a,*], Sifeng Bi [b], Matteo Broggi [a], Michael Beer [a,c,d]

[a] *Leibniz Universität Hannover, Institute for Risk and Reliability, Hannover, Germany*
[b] *University of Strathclyde, Department of Mechanical & Aerospace Engineering, Aerospace Centre of Excellence, Glasgow, United Kingdom*
[c] *University of Liverpool, Institute for Risk and Uncertainty, Liverpool, United Kingdom*
[d] *Tongji University, International Joint Research Center for Resilient Infrastructure & International Joint Research Center for Engineering Reliability and Stochastic Mechanics, Shanghai, China*
* Correspondence author. E-mail address: masaru.kitahara@irz.uni-hannover.de (M. Kitahara).

Abstract: This work proposes a distribution-free stochastic model updating framework to calibrate the joint probabilistic distribution of the multivariate correlated parameters. In this framework, the marginal distributions are defined as the staircase density functions and the correlation structure is described by the Gaussian copula function. The first four moments of the staircase density functions and the correlation coefficients are updated by an approximate Bayesian computation, in which the Bhattacharyya distance-based metric is proposed to define an approximate likelihood that is capable of capturing the stochastic discrepancy between model outputs and observations. The feasibility of the framework is demonstrated on two illustrative examples and a followed engineering application to the updating of a nonlinear dynamic system using observed time signals. The results demonstrate the capability of the proposed updating procedure in the very challenging condition where the prior knowledge about the distribution of the parameters is extremely limited (i.e., no information on the marginal distribution families and correlation structure is available).

Keywords:
Uncertainty quantification; Bayesian model updating; Staircase density function; Gaussian copula function; Bhattacharyya distance

1. Introduction

The model updating has been developed as a fascinating technique to mitigate the discrepancy between model outputs and experimental measurements [1,2]. The causes of the discrepancy during the model updating can be generally classified into following three categories:

- Parameter uncertainty. Model parameters, e.g., geometry dimensions, boundary conditions, and material properties, often cannot be exactly determined;
- Modelling uncertainty. Simplifications or approximations, e.g., linearization and frictionless mechanical joints, have to be made to numerically represent the physical system;
- Measurement uncertainty. Measured quantities are inevitably contaminated by the hard-to-control randomnesses, e.g., environmental noises and measurement system errors.

The deterministic model updating, especially for the sensitivity method [1], might be one of the most successful model updating techniques. It aims at calibrating the model parameters to find their optimal values from a single set of measurements. It has been employed in a wide range of practical applications e.g., the calibration of large-scale finite element (FE) models [3,4]. However, it considers measurement data as an exactly determined values/signals, ignoring the measurement uncertainty.

Comparatively, the stochastic model updating, including the perturbation method [5,6], Monte Carlo method [7,8], and Bayesian method [2,9], can be interpreted as the techniques to calibrate not the parameters themselves but the uncertainty characteristics, i.e., probabilistic distributions, so that the model outputs are committed not to the maximum fidelity to a single set of measurements but to the uncertainty characteristics of the multiple sets of measurements. In the stochastic model updating, uncertainty quantification (UQ) metrics play a key role to quantify the statistical discrepancy between the model outputs and measurements because of the above three sources of uncertainty. A series of distances, such as the Euclidian distance, Mahalanobis distance, and Bhattacharyya distance has been successfully proposed to define the UQ metrics in the stochastic model updating [8]. In addition, the Frobenius norm has been also utilized to define the UQ metric to quantify the difference between the covariance matrices of the model outputs and measurements [10]. Bi et al. [11] has recently developed a Bayesian updating framework employing the approximate Bayesian computation (ABC) technique [12,13], where the Bhattacharyya distance-based approximate likelihood is used. This framework has been demonstrated to be capable to calibrate numerical models such that the model outputs recreate wholly the uncertainty characteristics of target measurements. The framework has been furthermore extended to the calibration of dynamic systems, so that the procedure enables to quantify wholly the uncertainty characteristics of the measured time signals [14].

In the stochastic model updating, distribution families of the parameters commonly need to be assigned a priori, then the prior distribution of the hyper-parameters such as means and variances is updated to the posterior distribution using the measurement data. The distribution families, however, are often unknown beforehand due to the scarce and/or incomplete available data for the parameters. The newly released NASA UQ challenge problem 2019 [15], for instance, requires a model calibration task in an extremely challenging condition that no distribution information of the aleatory parameters is provided other than a common bounded support domain. In such situation, the assumption on the distribution formats might significantly affect the model updating results. Therefore, Kitahara et al. [16] has recently developed a distribution-free Bayesian updating framework, where staircase density functions [17] are assigned to the underlying distribution families of the parameters. Staircase density functions enable to flexibly approximate a broad range of distributions arbitrary close, such as highly skewed and/or multi-modal distributions, and are hence particularly appropriate to characterize the parameters whose density formats cannot be specified. The framework has been demonstrated to be capable of calibrating the probabilistic distribution of the parameters without limiting hypotheses on the distribution families.

Nevertheless, the aforementioned distribution-free updating framework still has open questions. Firstly, the framework has been currently only demonstrated on the updating by scalar-valued modal responses. Hence, in this study, it is extended to the updating of dynamic systems by measured time signals. Secondly, staircase density functions are provided for univariate random variables, and thus cannot consider the parameter dependencies, which might lead to inaccurate updating results in the presence of strong correlation among parameters. Copula functions are well-known to be capable to provide an effective way to characterize the dependence structure among parameters, and have been widely applied to reliability problems [18-20]. Among various types of copula functions, the Gaussian copula function is most widely used because it can be easily generalized to the multivariate case, and this property is particularly attractive for the stochastic model updating problem, in which very large number of parameters is considered as random variables.

The objective of this work is consequently to develop a stochastic model updating framework to calibrate the joint probability distribution of the correlated parameters without prior knowledge on the distribution families of the marginal distributions. In order to achieve this task, it is assumed that the joint probability distribution of the parameters is characterized by a combination of the Gaussian copula function and staircase density functions. Moment constraints for the existence of the staircase density functions and the correlation coefficient constraint for the existence of the copula function are then derived. Furthermore, the Bhattacharyya distance is utilized to define an approximate likelihood function quantifying the stochastic discrepancy between the model outputs and measurements, such that the hyper-parameters of the staircase density functions as well as the correlation coefficients of the copula function are calibrated through an ABC updating approach. The proposed framework is first demonstrated on both bi-variate and multi-variate cases using two simple illustrative examples, and then applied to a model updating problem of a seismic-isolated bridge pier model based on the simulated seismic response data, so as to demonstrate the feasibility of the framework in the updating of nonlinear dynamic systems.

The structure of this paper is as follows. Section 2 first describes theoretical and methodological bases of the three key ingredients of the proposed framework, i.e., the Bhattacharyya distance-based UQ metrics, staircase density functions, and Gaussian copula function. Then, in Section 3, we outline the formulation of the Bayesian updating with the combination of the Gaussian copula function and staircase density functions, and the proposed ABC updating framework. Illustrative applications are provided in Section 4, employing a simple shear building model and a spring-mass system, and the feasibility of the proposed framework in the updating of nonlinear dynamic systems by the measured time signals is further demonstrated in Section 5. Finally, Section 6 gives conclusions to this paper.

2. Theories and methodologies

2.1. Bhattacharyya distance-based UQ metrics

The system under investigation in the stochastic model updating is described as:

$$\boldsymbol{y} = h(\boldsymbol{x}) \tag{1}$$

where $\boldsymbol{x} = [x_1, x_2, \cdots, x_n]$ denotes a row vector of n input parameters; $\boldsymbol{y} = [y_1, y_2, \cdots, y_m]$ means a row vector of m output features; $h(\cdot)$ means the simulator. The output features herein can be either scalar-valued modal responses or time signals. In the latter case, $\boldsymbol{y}$ is replaced to be $\mathbf{y} = [\boldsymbol{y}_1, \boldsymbol{y}_2, \cdots, \boldsymbol{y}_m]$, with $\boldsymbol{y}_i = [y_i(0), y_i(1), \cdots, y_i(t)]^T$, $\forall i = 1, 2, \cdots, m$, where t indicates the time parameter. The simulator $h(\cdot)$ can be either high-fidelity models, e.g., FE models, or surrogate models.

Uncertainties involved in the system are first characterized by representing the input parameters as random variables, and are then propagated through the simulator to the output features. This can be typically achieved by randomly generating the multiple sets of the parameters and corresponding output features. Let the sample size be N_{sim}, the simulator h is evaluated N_{sim} times for obtaining the sample set of the simulated features $\mathbf{Y}_{\text{sim}} \in \mathbb{R}^{N_{\text{sim}} \times m}$:

$$\mathbf{Y}_{\text{sim}} = \left[\mathbf{y}^{(1)}, \mathbf{y}^{(2)}, \cdots, \mathbf{y}^{(N_{\text{sim}})}\right]^T, \text{with } \mathbf{y}^{(k)} = \left[y_1^{(k)}, y_2^{(k)}, \cdots, y_m^{(k)}\right], \forall k = 1, 2, \cdots, N_{\text{sim}} \tag{2}$$

in the case that the output features are given as the modal responses. $\mathbf{Y}_{\text{sim}}$ can be simply extended to $\mathbf{Y}_{\text{sim}} \in \mathbb{R}^{N_{\text{sim}} \times m \times (t+1)}$ for the time signals case.

In addition to the simulated features, corresponding observed features are also necessary in the model updating. Let the number of observations be N_{obs}, the sample set of the observed features $\mathbf{Y}_{\text{obs}}$ possesses a same structure as Eq. (2), but only the number of rows is changed from N_{sim} to N_{obs}. The stochastic model updating is then aimed at minimizing the stochastic discrepancy between $\mathbf{Y}_{\text{sim}}$ and $\mathbf{Y}_{\text{obs}}$ by calibrating the joint probability distribution of the parameters.

To quantify the discrepancy between $\mathbf{Y}_{\text{sim}}$ and $\mathbf{Y}_{\text{obs}}$, the Bhattacharyya distance-based UQ metric is employed in this study. The original definition of the Bhattacharyya distance is given as [21]:

$$d_B(\mathbf{Y}_{\text{sim}}, \mathbf{Y}_{\text{obs}}) = -\log\left[\int_{\mathbb{y}} \sqrt{f_{\mathbf{Y}_{\text{sim}}}(\boldsymbol{y}) f_{\mathbf{Y}_{\text{obs}}}(\boldsymbol{y})}\, \mathrm{d}\boldsymbol{y}\right] \tag{3}$$

where $f_{(\cdot)}(\boldsymbol{y})$ means the probability density function (PDF) of the output features $\boldsymbol{y}$; $\mathbb{y}$ is the support domain of the output features which comprises m-dimensional space for the modal responses but the $\{m \times (t+1)\}$-dimensional space for the time signals. Eq. (3) indicates the Bhattacharyya distance is a measure of the overlap between the two probability distributions. Hence, it is capable to consider not only mean information but whole statistical information of two different sample sets. However, the direct evaluation of Eq. (3) is usually impractical since precisely estimating the joint PDF of the output features is non-trivial due to the necessity of time-consuming repeated model evaluations or the very limited number of available measurement data. To overcome this issue, Bi et al. [11] proposed the so-called binning algorithm to evaluate the probability mass function (PMF) of the given sample sets, so that the discrete Bhattacharyya distance is utilized instead [22]:

$$d_B(\mathbf{Y}_{\text{sim}}, \mathbf{Y}_{\text{obs}}) = -\log\left\{\sum_{j=1}^{N_{\text{bin}}} \sqrt{P_{\mathbf{Y}_{\text{sim}}}^{(j)} P_{\mathbf{Y}_{\text{obs}}}^{(j)}}\right\} \tag{4}$$

where $N_{\rm bin}$ denotes the total number of bins; $P_{(\cdot)}^{(j)}$ denotes the PMF value of the output features at the jth bin. In the binning algorithm, a grid is created in the whole support domain of the output features, and thus the total number of bins would be $N_{\rm bin} = n_{\rm bin}^{m}$ for the modal responses and $N_{\rm bin} = n_{\rm bin}^{m\times(t+1)}$ for the time signals, where $n_{\rm bin}$ indicates the number of bins for each output feature. One can refer to Ref. [11] for the detailed procedure of the binning algorithm. The discrete Bhattacharyya distance has been demonstrated to be effective in relatively low-dimensional problems (e.g., the dimension is less than six).

On the other hand, even the evaluation of Eq. (4) is still impractical for the very high-dimensional problems where the output features comprise time signals, since the number of bins is exponentially increasing with the number of dimensions because of the so-called curse of dimensionality. To tackle this issue, Kitahara et al. [14] has proposed a dimension reduction procedure to use the Bhattacharyya distance for the comparison of two different time signals, consisting of the following steps:

1) Define the common window length L for $\mathbf{Y}_{\rm sim}$ and $\mathbf{Y}_{\rm obs}$. Divide them into three-dimensional sub-arrays $\mathbf{Y}_{\rm sim}^{s} \in \mathbb{R}^{N_{\rm sim}\times m\times \rm L}$ and $\mathbf{Y}_{\rm obs}^{s} \in \mathbb{R}^{N_{\rm obs}\times m\times \rm L}$, $\forall s = 1,\cdots,\lfloor(t+1)/\mathrm{L}\rfloor$, where $\lfloor\cdot\rfloor$ denotes the lower integer of the investigated values;
2) Compute the root mean square (RMS) matrices $\mathbf{R}_{\mathbf{Y}_{\rm sim}}^{s} \in \mathbb{R}^{N_{\rm sim}\times m}$ of each sub-array $\mathbf{Y}_{\rm sim}^{s}$ along its third dimension and obtain the sample set of the RMS values $\mathbf{R}_{\mathbf{Y}_{\rm sim}} \in \mathbb{R}^{N_{\rm sim}\times m\times\lfloor(t+1)/\mathrm{L}\rfloor}$. Do similar procedure for the observed features and obtain $\mathbf{R}_{\mathbf{Y}_{\rm obs}} \in \mathbb{R}^{N_{\rm obs}\times m\times\lfloor(t+1)/\mathrm{L}\rfloor}$;
3) Evaluate in total $\lfloor(t+1)/\mathrm{L}\rfloor$ Bhattacharyya distances d_B^s between two sample sets $\mathbf{R}_{\mathbf{Y}_{\rm sim}}^{s}$ and $\mathbf{R}_{\mathbf{Y}_{\rm obs}}^{s}$ using Eq. (4);
4) Employ the RMS value of the set of the Bhattacharyya distances, R_{d_B}, as the UQ metric.

The authors' experience shows that $\mathrm{L} = (0.02{\sim}0.03)\cdot t$ is the reasonable choice for the window length L, and such choice indicates that each window contains 2~3 % of the time signals. As such, the time signals are degraded to a series of RMS values. The above defined Bhattacharyya distance-based UQ metric has been demonstrated to be able to quantify the uncertainty characteristics of the entire time signals [14].

2.2. Staircase density functions

Let the input parameter x_i, $\forall i = 1,\cdots,n$, be a random variable having the support domain $[\underline{x}_i, \overline{x}_i]$ and a quadruple of the hyper-parameters $\boldsymbol{\theta}_{x_i} = [\mu_i, m_{2i}, \tilde{m}_{3i}, \tilde{m}_{4i}]$ consisting of the mean μ_i, variance m_{2i}, skewness $\tilde{m}_{3i}$, and kurtosis $\tilde{m}_{4i}$. The skewness $\tilde{m}_{3i}$ and kurtosis $\tilde{m}_{4i}$ are defined as ratios of the variance to the third and fourth central moments by $\tilde{m}_{3i} = m_{3i}/m_{2i}^{3/2}$ and $\tilde{m}_{4i} = m_{4i}/m_{2i}^{2}$, respectively. The feasibility condition for the existence of x_i can be defined as moment constraints given by a series of inequalities $\Theta_i = \{\boldsymbol{\theta}_{x_i} : g(\boldsymbol{\theta}_{x_i}) \le 0\}$, and their components are summarized in Table 1 [23,24].

Table 1. Moment constraints for the existence of staircase density functions.

Hyper-parameters	Moment constraints
Mean μ_i	$g_1 = \underline{x}_i - \mu_i$
	$g_2 = \mu_i - \overline{x}_i$
Variance m_{2i}	$g_3 = -m_{2i}$
	$g_4 = m_{2i} - v_i$
Skewness $\tilde{m}_{3i}$	$g_5 = m_{2i}^2 - m_{2i}(\mu_i - \underline{x}_i)^2 - \tilde{m}_{3i}m_{2i}^{3/2}(\mu_i - \underline{x}_i)$
	$g_6 = \tilde{m}_{3i}m_{2i}^{3/2}(\overline{x}_i - \mu_i) - m_{2i}(\overline{x}_i - \mu_i)^2 + m_{2i}^2$
	$g_7 = 4m_{2i}^2 + \tilde{m}_{3i}^2 m_{2i}^3 - m_{2i}^2(\overline{x}_i - \underline{x}_i)^2$
	$g_8 = 6\sqrt{3}\tilde{m}_{3i}m_{2i}^{3/2} - (\overline{x}_i - \underline{x}_i)^3$
	$g_9 = -6\sqrt{3}\tilde{m}_{3i}m_{2i}^{3/2} - (\overline{x}_i - \underline{x}_i)^3$
Kurtosis $\tilde{m}_{4i}$	$g_{10} = -\tilde{m}_{4i}m_{2i}^2$
	$g_{11} = 12\tilde{m}_{4i}m_{2i}^2 - (\overline{x}_i - \underline{x}_i)^4$
	$g_{12} = \left(\tilde{m}_{4i}m_{2i}^2 - v_i m_{2i} - u_i\tilde{m}_{3i}m_{2i}^{3/2}\right)(v_i - m_{2i}) + \left(\tilde{m}_{3i}m_{2i}^{3/2} - \mu_i m_{2i}\right)^2$
	$g_{13} = \tilde{m}_{3i}^2 m_{2i}^3 + m_{2i}^3 - \tilde{m}_{4i}m_{2i}^3$

[a] $u_i = \underline{x}_i + \overline{x}_i - 2\mu_i$ and $v_i = (\mu_i - \underline{x}_i)(\overline{x}_i - \mu_i)$.

Let the bounded support domain $[\underline{x}_i, \overline{x}_i]$ equally partitioned into n_b subintervals with the length $\kappa = (\overline{x}_i - \underline{x}_i)/n_b$, x_i can be considered as a staircase random variable, and then its PDF $f_{x_i}(x)$ can be expressed as [17]:

$$f_{x_i}(x) = \begin{cases} l^j & \forall x \in (x_i^j, x_i^{j+1}], \forall j = 1, 2, \cdots, n_b \\ 0 & \text{otherwise} \end{cases} \tag{5}$$

where l^j is the PDF value of the jth bin; $x_i^j = \underline{x}_i + (j-1)\kappa$ is the left partitioning point of the jth bin. It is noted that l^j holds that $l^j \geq 0$ for all the bins and $\kappa \sum_{j=1}^{n_b} l^j = 1$. The PDF values $\boldsymbol{l}_i$ are derived by solving the following optimization problem [17]:

$$\hat{\boldsymbol{l}}_i = \underset{\boldsymbol{l} \geq 0}{\operatorname{argmin}} \left\{ J(\boldsymbol{l}) \colon \sum_{j=1}^{n_b} \int_{x_i^j}^{x_i^{j+1}} x l^j dx = \mu_i, \sum_{j=1}^{n_b} \int_{x_i^j}^{x_i^{j+1}} (x - \mu_i)^r l^j dx = m_{ri}, r = 2, 3, 4 \right\} \tag{6}$$

where $J(\cdot)$ is an arbitrary selected cost function expressed as:

$$J(\boldsymbol{l}) = \boldsymbol{l}^T \mathbf{I} \boldsymbol{l} \tag{7}$$

where $\mathbf{I}$ means the identity matrix. This cost function leads to the resultant staircase random variables minimizing the squared sum of the likelihood at each bin. Based on the moment matching constraints, Eq. (6) can be written as [17]:

$$\hat{\boldsymbol{l}}_i = \underset{\boldsymbol{l} \geq 0}{\operatorname{argmin}} \left\{ J(\boldsymbol{l}) \colon \mathbf{A}(\boldsymbol{\theta}_{x_i}, n_b) \boldsymbol{l} = \boldsymbol{b}(\boldsymbol{\theta}_{x_i}), \boldsymbol{\theta}_{x_i} \in \Theta_i \right\} \tag{8}$$

where

$$\mathbf{A} = \begin{bmatrix} \kappa \boldsymbol{e} \\ \kappa \boldsymbol{c} \\ \kappa \boldsymbol{c}^2 + \kappa^3/12 \\ \kappa \boldsymbol{c}^3 + \kappa^3 \boldsymbol{c}/4 \\ \kappa \boldsymbol{c}^4 + \kappa^3 \boldsymbol{c}^2/2 + \kappa^5/80 \end{bmatrix}, \text{and } \boldsymbol{b} = \begin{bmatrix} 1 \\ \mu_i \\ \mu_i^2 + m_{2i} \\ \widetilde{m}_{3i} m_{2i}^{3/2} + 3\mu_i m_{2i} + \mu_i^3 \\ m_{4i} m_{2i}^2 + 4\widetilde{m}_{3i} m_{2i}^{3/2} \mu_i + 6 m_{2i} \mu_i^2 + \mu_i^4 \end{bmatrix}$$

where $\boldsymbol{c}$ means a column vector of the centre of the bin $c_j = (x_i^j + x_i^{j+1})/2$; $\boldsymbol{c}^n$ denotes the component wise nth power of $\boldsymbol{c}$; $\boldsymbol{e}$ refers to a vector of ones.

The convexity of the optimization problem in Eq. (8) enables the fast computation of the staircase density heights. In addition, a relatively small value of n_b (e.g., $n_b = 25 \sim 50$) is enough for obtaining practically smooth distribution shapes for the PMF evaluation, which makes the computation further faster. These features are particularly appropriate for the stochastic updating, where the tremendous number of computations of the probability distributions is necessary. Furthermore, staircase density functions enable to flexibly approximate a broad range of distributions arbitrary close, such as highly skewed and/or multi-modal distributions. Therefore, they can serve as a distribution-free uncertainty characterization model of the parameters whose distribution families cannot be determined.

2.3. Gaussian copula function

Copula functions couple the multivariate joint cumulative distribution function (CDF) with its one-dimensional marginal CDFs. Conversely, copula functions are also seen as the multivariate joint CDFs whose one-dimensional marginal CDFs follow a uniform distribution on the interval of [0, 1]. According to Sklar's theorem [25], the bivariate joint CDF of two random variables x_1 and x_2 can be expressed as:

$$F_{\mathbf{x}}(x_1, x_2) = C\left(F_{x_1}(x_1), F_{x_2}(x_2)\right) \tag{9}$$

where $F_{x_1}(x_1)$ and $F_{x_2}(x_2)$ are the marginal CDFs of x_1 and x_2, respectively; $C\left(F_{x_1}(x_1), F_{x_2}(x_2)\right)$ is the copula function. From Eq. (9), the bivariate joint PDF of x_1 and x_2 is then written as:

$$f_{\mathbf{x}}(x_1, x_2) = c\left(F_{x_1}(x_1), F_{x_2}(x_2)\right) f_{x_1}(x_1) f_{x_2}(x_2) \tag{10}$$

where $c\left(F_{x_1}(x_1), F_{x_2}(x_2)\right)$ denotes the copula density function given as:

$$c\left(F_{x_1}(x_1), F_{x_2}(x_2)\right) = c(u_1, u_2) = \frac{\partial^2 c(u_1, u_2)}{\partial u_1 \partial u_2} \quad (11)$$

Theoretically, the joint distribution of x_1 and x_2 can be fully and uniquely represented by Eqs. (9) and (10) if the marginal distributions of x_1 and x_2, and the copula function are given.

There are many copula function types in the literature, including the Gaussian, t, Frank, Gumbel, and Clayton copula functions. They are characterized by their own dependence structures. The latter three types of copula function can be referred to as Archimedean copulas. The Archimedean copulas have only a single parameter, and thus cannot provide the general dependence structure among more than two random variables. Alternatively, the general dependence structure is often modeled by the pair-copula decomposition introduced as a canonical vine copula [26]. Conversely, the Gaussian and t copulas, which belong to elliptical copulas, can be straightforwardly generalized to the multivariate case. Particularly, the Gaussian copula function is most widely used since it only needs the correlation matrix to determine the dependence structure.

In this study, the joint probability distribution of the input parameters $\boldsymbol{x}$ is finally characterized by the combination of the Gaussian copula function and staircase density functions as:

$$\begin{aligned} F_{\mathbf{x}}(\boldsymbol{x}) &= C_G\left(F_{x_1}(x_1), F_{x_2}(x_2), \cdots, F_{x_n}(x_n); \boldsymbol{\rho}\right) \\ &= \Phi_\rho\left(\Phi^{-1}\left(F_{x_1}(x_1)\right), \Phi^{-1}\left(F_{x_2}(x_2)\right), \cdots, \Phi^{-1}\left(F_{x_n}(x_n)\right)\right) \end{aligned} \quad (12)$$

where C_G indicates the Gaussian copula function; $\boldsymbol{\rho}$ indicates the correlation matrix; Φ_ρ indicates the multivariate standard normal CDF with $\boldsymbol{\rho}$; Φ^{-1} indicates the inverse function of the standard normal CDF. It is noted that each marginal CDF $F_{x_i}(x_i)$ can be described by the empirical CDF of the staircase density function $f_{x_i}(\cdot)$, for $i = 1,2,\cdots,n$. The correlation matrix $\boldsymbol{\rho}$ can be expressed as:

$$\boldsymbol{\rho} = \begin{bmatrix} 1 & \rho_{12} & \rho_{13} & \cdots & \rho_{1n} \\ \rho_{12} & 1 & \rho_{23} & \cdots & \rho_{2n} \\ \rho_{13} & \rho_{23} & \ddots & \cdots & \vdots \\ \vdots & \vdots & \vdots & 1 & \rho_{n-1n} \\ \rho_{1n} & \rho_{2n} & \cdots & \rho_{n-1n} & 1 \end{bmatrix} \quad (13)$$

where ρ_{ij}, for $i = 1,2,\cdots,n-1$ and $j = i+1,\cdots,n$, means the correlation coefficient. The range of each correlation coefficient can reach [-1, 1]. The correlation matrix $\boldsymbol{\rho}$ should be the symmetric and positive semi-definite matrix. Hence, the feasibility condition for the existence of the Gaussian copula function can be defined by the correlation coefficient constraint $\mathcal{P} = \{\boldsymbol{\rho}: \mathrm{chol}(\boldsymbol{\rho}) \neq \emptyset\}$, where $\mathrm{chol}(\cdot)$ means the Cholesky factorization.

3. Distribution-free stochastic model updating

3.1. Bayesian model updating of the joint probabilistic distribution

In the proposed stochastic updating framework, the well-known Bayesian inference is utilized. It is based on the Bayes' theorem [27]:

$$P(\boldsymbol{\vartheta}|\mathbf{Y}_{\text{obs}}) = \frac{P_L(\mathbf{Y}_{\text{obs}}|\boldsymbol{\vartheta})P(\boldsymbol{\vartheta})}{P(\mathbf{Y}_{\text{obs}})} \quad (14)$$

where $P(\boldsymbol{\vartheta})$ denotes the prior PDF of the parameters to be inferred $\boldsymbol{\vartheta}$ that is determined by the initial knowledge of the system and expert judgement; $P(\boldsymbol{\vartheta}|\mathbf{Y}_{\text{obs}})$ means the posterior PDF of $\boldsymbol{\vartheta}$ conditional to the measurements, representing the updated knowledge of $\boldsymbol{\vartheta}$; $P(\mathbf{Y}_{\text{obs}})$ indicates the normalization factor (evidence) ensuring the integral of the posterior distribution equal to one; $P_L(\mathbf{Y}_{\text{obs}}|\boldsymbol{\theta})$ indicates the likelihood function of $\mathbf{Y}_{\text{obs}}$ that is defined as the PDF values of the measurements conditional to each instance of $\boldsymbol{\vartheta}$.

To calibrate the joint probabilistic distribution of the parameters $\boldsymbol{x}$ given by Eq. (13), the hyper-parameters of the staircase density functions $\boldsymbol{\theta}_{x_i}$, for $i = 1,\cdots,n$, and the correlation coefficients of the Gaussian copula function ρ_{ij}, for $i = 1,\cdots,n-1$ and $j = i+1,\cdots,n$, are considered to be the inferred parameters $\boldsymbol{\vartheta}$. Based on the moment constraints Θ_i, the support domains of $\boldsymbol{\theta}_{x_i}$ can be determined as:

$$\mu_i \in [\underline{x}_i, \overline{x}_i], m_{2i} \in \left[0, \frac{(\overline{x}_i - \underline{x}_i)^2}{4}\right], m_{3i} \in \left[-\frac{(\overline{x}_i - \underline{x}_i)^3}{6\sqrt{3}}, \frac{(\overline{x}_i - \underline{x}_i)^3}{6\sqrt{3}}\right], m_{4i} \in \left[0, \frac{(\overline{x}_i - \underline{x}_i)^4}{12}\right] \tag{15}$$

It is noted that the support domains are defined not for the skewness and kurtosis but the third and fourth central moments, since the skewness and kurtosis are conditional on the variance. On the other hand, the support domain of ρ_{ij} is simply defined as [-1, 1]. In this study, it is assumed all parameters to be inferred are independent. Based on these support domains with the moment constraints Θ_i and correlation coefficient constraint P, the prior PDF $P(\boldsymbol{\vartheta})$ can be expressed as:

$$P(\boldsymbol{\vartheta}) = \prod_{i=1}^{n} P(\boldsymbol{\theta}_{x_i}) I_{\Theta_i}(\boldsymbol{\theta}_{x_i}) \cdot \prod_{i=1}^{n-1} \prod_{j=i+1}^{n} P(\rho_{ij}) I_{\mathcal{P}}(\rho_{ij}) \tag{16}$$

where $P(\boldsymbol{\theta}_{x_i})$ and $P(\rho_{ij})$ indicate the prior PDFs of the hyper-parameters and correlation coefficients that are chosen as the uniform distributions on their respective support domains; $I_{\Theta_i}(\boldsymbol{\theta}_{x_i})$ denotes the indicator function of $\boldsymbol{\theta}_{x_i}$, which equals to one if Θ_i is satisfied and otherwise equals to zero; $I_{\mathcal{P}}(\rho_{ij})$ is similarly the indicator function of ρ_{ij}. As such, the proposed stochastic updating framework requires only assumptions on the support domains of the input parameters $\boldsymbol{x}$.

This brings totally $4n + n(n-1)/2$ inferred parameters. However, it is widely recognized that the direct evaluation of the posterior PDF over such a high-dimensional parameter space is not trivial [28]. Hence, the well-known advanced sampling technique, termed transitional Markov chain Monte Carlo (TMCMC) [29], is employed in this study. TMCMC is a sequential procedure sampling from a series of transitional PDFs that will gradually converge to the actual posterior PDF, thus it enables to generate samples from the very complex posterior PDF. One can refer to Refs. [29,30] for more details of the TMCMC algorithm.

3.2. Approximate Bayesian computation

The likelihood function plays a key role in the Bayesian model updating. Utilizing the Bayesian inference in the stochastic updating results in the following theoretical likelihood function:

$$P_L(\mathbf{Y}_{\text{obs}}|\boldsymbol{\vartheta}) = \prod_{k=1}^{N_{\text{obs}}} P(\mathbf{Y}_{\text{obs}}^{(k)}|\boldsymbol{\vartheta}) \tag{17}$$

where $P(\mathbf{Y}_{\text{obs}}^{(k)}|\boldsymbol{\vartheta})$ means the PDF value of the kth observations $\mathbf{Y}_{\text{obs}}^{(k)}$ conditional to each instance of the inferred parameters $\boldsymbol{\vartheta}$. The direct evaluation of Eq. (17), however, is often impractical since it requires the significant number of model evaluations so as to precisely estimate the PDFs of the corresponding model outputs.

The ABC method [12,13] has been successfully employed to overcome this obstacle by replacing the above full likelihood function with an approximate but efficient likelihood function that contains information of both the measurements and inferred parameters $\boldsymbol{\vartheta}$. Various forms of the approximate likelihood functions have been investigated in the literature, such as the Gaussian [31], Epanechnikov [32], and inverse squared error [33] functions. Regardless of the function form, it is essential to utilize the comprehensive UQ metric which can serve as an effective connection between the measurements and inferred parameters. In this study, an approximate likelihood function by the Gaussian function is defined by utilizing the Bhattacharyya distance-based UQ metric as:

$$P_L(\mathbf{Y}_{\text{obs}}|\boldsymbol{\vartheta}) \propto exp\left\{-\frac{d_B^2}{\varepsilon^2}\right\} \tag{18}$$

where ε is the pre-defined width factor, which controls the centralization degree of the posterior PDF. A smaller ε provides a more peaked posterior PDF, which is more likely to converge to its true value but needs more computation cost for convergence. Hence, its choice is based on specific applications, while it is recommended to be within the interval of $[10^{-3}, 10^{-1}]$ [31]. By utilizing the Bhattacharyya distance (or the RMS value R_{d_B} for the time signals case), the proposed likelihood enables to quantify the comprehensive uncertainty characteristics of the model outputs and measurements.

The schematic in Fig. 1 illustrates overall framework of the proposed distribution-free stochastic updating procedure. As already mentioned, only the support domains of the parameters are required to perform this framework. Sampling from the prior PDF in Eq. (16) can be achieved by the rejection sampling. TMCMC is then utilized to update the inferred parameters to the posterior PDF using the Bhattacharyya distance-based approximate likelihood. By assigning most probable values (MPVs) of the posterior PDF, the joint probabilistic distribution of the input parameters is finally calibrated such that the stochastic model outputs generated from the joint distribution is capable to recreate wholly the uncertainty characteristics of the target measurements. It is important to note that, the calibrated distribution of the parameters is not necessarily applicable to the reliability analysis so as to estimate the probabilities of rare events, since the parameters are finitely bounded due to the definition of the staircase density functions and a domain where the rare event happens might be excluded.

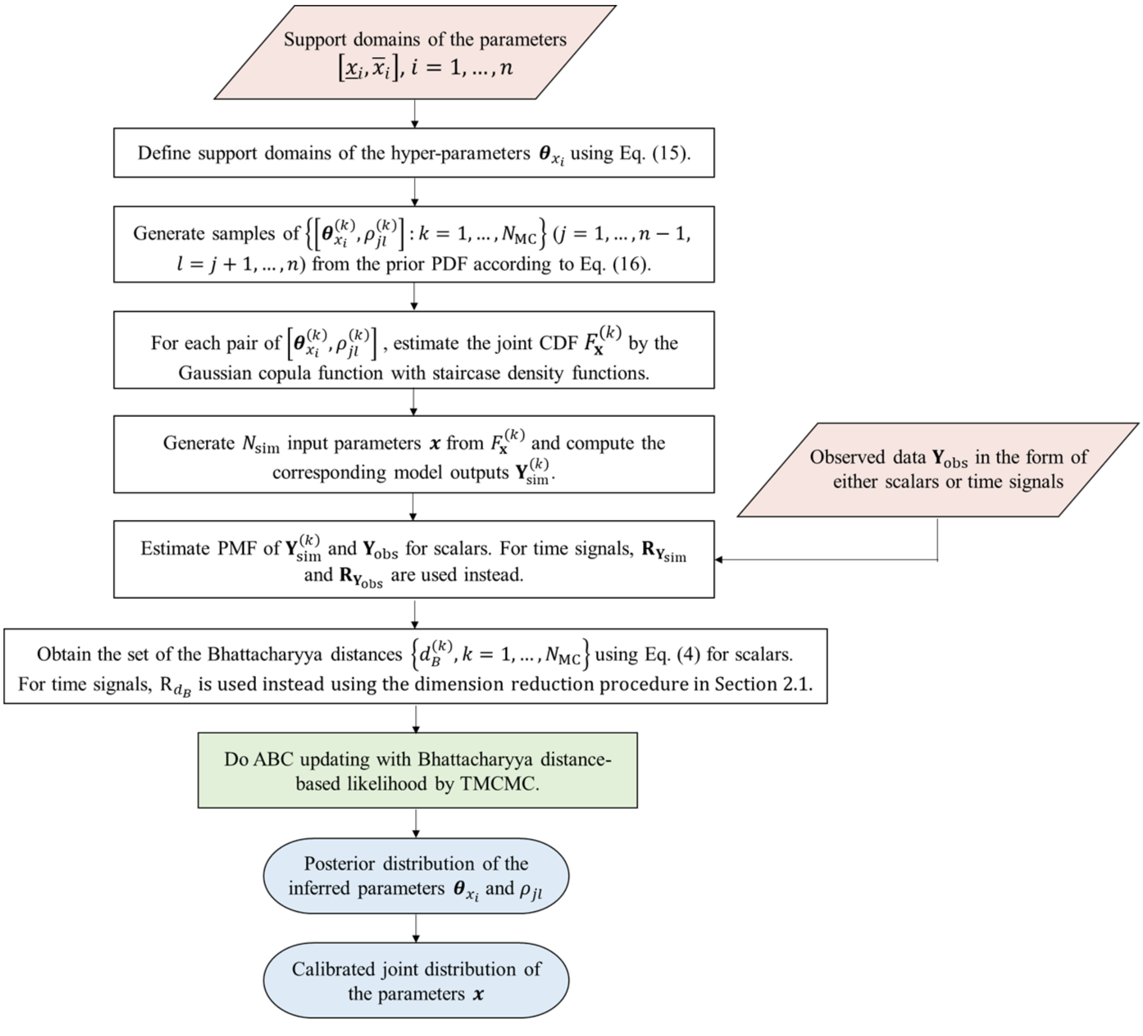

Fig. 1. Schematic of the proposed stochastic model updating framework.

4. Principle and illustrative applications

4.1. Case study I: The two degree of freedom shear building model

The first case study is performed on a two degree of freedom (DOF) shear building model given in Fig. 2(a). This case study aims at demonstrating the feasibility of the proposed updating procedure for illustrative bivariate case, and how the stochastic model updating fails by ignoring the parameter dependency. This model has been initially introduced by Ref. [28], where the first and second story masses are considered as the fixed values with $m_1 = 16.531 \times 10^3$ kg and $m_2 = 16.131 \times 10^3$ kg. On the other hand, the first and second interstory stiffnesses are characterized as $k_1 = \overline{k}x_1$ and $k_2 = \overline{k}x_2$, where $\boldsymbol{x} = [x_1, x_2]$ indicates the inferred parameters, and $\overline{k} = 29.7 \times 10^6$ N/m is the nominal value.

In Ref. [28], the prior PDF $P(\boldsymbol{x})$ is determined by the pair of uncorrelated lognormal distributions with the MPVs 1.3 and 0.8 for x_1 and x_2, respectively, and the unit standard deviations. By employing the first two natural frequencies $\tilde{f}_1 = 4.31$ Hz and $\tilde{f}_2 = 9.83$ Hz as the observed features, the posterior PDF $P(\boldsymbol{x}|\mathbf{Y}_{\text{obs}})$ is expressed as:

$$P\left(\boldsymbol{x}\middle|\left[\tilde{f}_1, \tilde{f}_2\right]\right) \propto exp\left[-\frac{M(\boldsymbol{x})}{2\sigma^2}\right] P(\boldsymbol{x}) \tag{19}$$

where $\sigma = 1/16$ indicates the standard deviation of the prediction error; $M(\cdot)$ is the modal measure-of-fit function expressed as:

$$M(\boldsymbol{x}) = \sum_{j=1}^{2} \lambda^2 \left[\frac{f_j^2(\boldsymbol{x})}{\tilde{f}_j^2} - 1\right]^2 \tag{20}$$

where $\lambda = 1$ is the weight; $f_j(\boldsymbol{x})$ denotes the jth natural frequency obtained as the model output. Fig. 2(b) illustrates the posterior distribution in Eq. (19). It can be seen that the posterior distribution has a clear negative correlation.

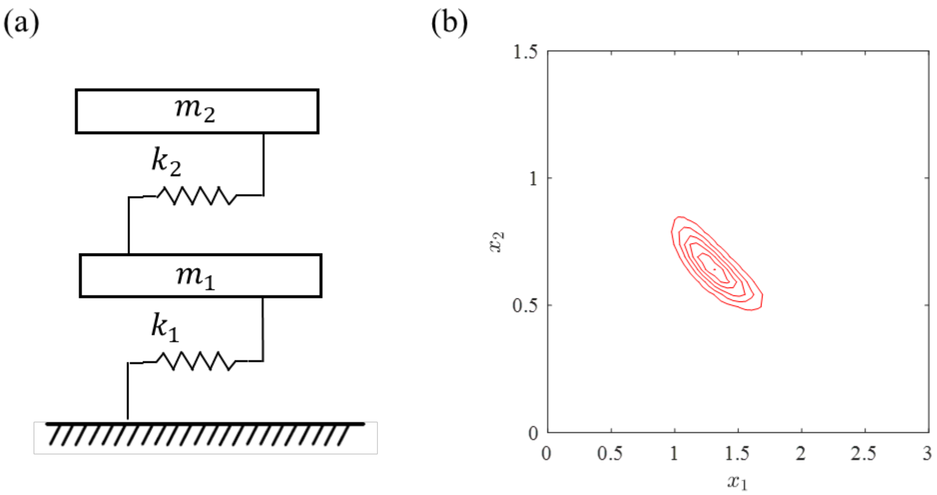

Fig. 2. (a) 2-DOF shear building model; (b) Posterior distribution in Eq. (19).

The aforementioned original problem can be interpreted to aim at estimating the set of plausible values of the input parameters $\boldsymbol{x}$ using the single set of observed features $\left[\tilde{f}_1, \tilde{f}_2\right]$ through the Bayesian scheme. Comparatively, the uncertainty characteristics of the input parameters and observed features are altered hereafter to perform the stochastic updating where the joint probability distribution of the input parameters, $F_{\mathbf{x}}(\boldsymbol{x})$, is calibrated using the multiple sets of the observed features. The target joint distribution is defined to be identical to the posterior distribution in Eq. (19). The number of observed features is set to be $N_{\text{obs}} = 100$; thus, N_{obs} sample sets of the input parameters are generated from the target distribution $P\left(\boldsymbol{x}\middle|\left[\tilde{f}_1, \tilde{f}_2\right]\right)$ utilizing TMCMC, and the corresponding observed features $\mathbf{Y}_{\text{obs}}$ are collected by evaluating the model with these sample sets. Note that the target distribution of the input parameters is unknown beforehand in actual. As such, the altered problem is aimed at calibrating the joint distribution of the input parameters to recreate wholly the uncertainty characteristics of $\mathbf{Y}_{\text{obs}}$ by the model outputs generated from the joint distribution.

The bounded support domains of x_1 and x_2 are determined as provided in Table 2. The support domain of the hyper-parameters $\boldsymbol{\theta}_{x_1}$ and $\boldsymbol{\theta}_{x_2}$ can be computed using Eq. (15). Let the sample size be $N_{\text{MC}} = 1000$, N_{MC} sets of the initial values of $\boldsymbol{\theta}_{x_1}$ and $\boldsymbol{\theta}_{x_2}$, maintaining the moment constraints Θ_1 and Θ_2, are generated by the rejection sampling while N_{MC} initial values of the correlation coefficient ρ_{12} are arbitrary generated from its support of [-1, 1]. For each set of $[\boldsymbol{\theta}_{x_1}, \boldsymbol{\theta}_{x_2}, \rho_{12}]$, the joint probability distribution of the input parameters $\boldsymbol{x}$ described by the Gaussian copula function with the marginal staircase density functions is determined. The number of bins in staircase density estimation is chosen as $n_b = 25$. At the same time, the number of simulated features is set to be $N_{\text{sim}} = 1000$; hence, N_{sim} sample sets of the input parameters $\boldsymbol{x}$ are generated from each joint distribution $\left\{F_{\mathbf{x}}^{(k)}: k = 1, \cdots, N_{\text{MC}}\right\}$.

The corresponding initial simulated features $\mathbf{Y}_{\mathrm{sim}}^{(k)}$ are then collected by evaluating the model for each sample sets of the input parameters. Arbitrary selected initial simulated features are plotted in Fig. 3, together with the target observed features. The figure clearly demonstrates the presence of significant discrepancy between the simulated and observed features, implying the necessity of stochastic model updating for better representation of the uncertainty characteristics of the observed features by means of the model outputs.

Table 2. Uncertainty characteristics of the 2-DOF model.

Parameter	Support domain	Target distribution
x_1	$x_1 \in [0, 3.0]$	The marginal distribution of Eq. (19)
x_2	$x_2 \in [0, 1.5]$	The marginal distribution of Eq. (19)

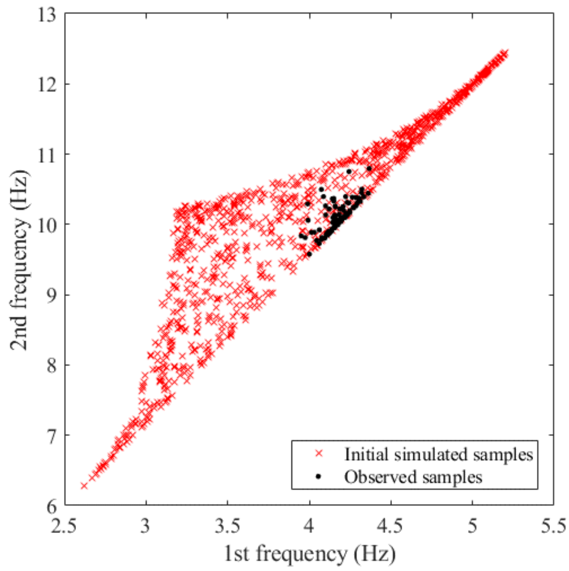

Fig. 3. Observed and initial simulated features.

The Bhattacharyya distance is estimated for each set of the simulated features $\mathbf{Y}_{\mathrm{sim}}^{(k)}$. The number of bins in the binning algorithm is chosen to be $n_{\mathrm{bin}} = 5$. Then, the Bayesian model updating of totally nine inferred parameters (i.e., the hyper-parameters $\boldsymbol{\theta}_{x_i} = \{\mu_i, m_{2i}, \tilde{m}_{3i}, \tilde{m}_{4i}\}$, for $i = 1, 2$, as well as the correlation coefficient ρ_{12}) is performed using the Bhattacharyya distance-based likelihood function. The width factor in the likelihood function is set to be $\varepsilon = 0.02$.

Fig. 4 shows the posterior PDFs of all the inferred parameters obtained after totally ten TMCMC iterations, together with their target and calibrated values. The target values are estimated based on samples generated from the target joint distribution, while the calibrated values are estimated as the MPVs of the posterior PDFs. These values are summarized in Table 3. It can be seen that the posterior PDFs of all the inferred parameters are significantly updated compared with their uniform priors that are identical to ranges of the horizontal axes of Fig. 4. Compared with the means and variances, the posterior supports of the skewnesses and kurtoses are, however, not reduced much from their prior supports, fulfilling the general experience that the higher order moments are difficult to be precisely updated compared with the means [34,35]. Nevertheless, the calibrated values including the kurtoses and the correlation coefficient are in good agreement with their target values with the largest relative error less than 6 %, except for the variance m_{21} and two skewnesses $\tilde{m}_{31}$ and $\tilde{m}_{32}$. The relative errors are shown as percentages in the parentheses after the calibrated values in Table 3. It is noted that, the large relative error in m_{21} can be explained to be caused by its quite small target value, and it is within an allowable limit to obtain the staircase density function approximating the target distribution as in Fig. 5. Meanwhile, the large errors in $\tilde{m}_{31}$ and $\tilde{m}_{32}$ are apparently caused by the wrongly identified signs, whereas their absolute values are close to those of the targets. It should be noted that, the signs of the skewnesses do not strongly affect the uncertainty characteristics of the output features as long as their absolute values are small such that the resultant distributions are almost symmetric. To this end, it is demonstrated that the Bhattacharyya distance can quantify not only mean information but also higher statistical information, i.e., the variances, skewnesses, and kurtoses as well as correlation coefficient.

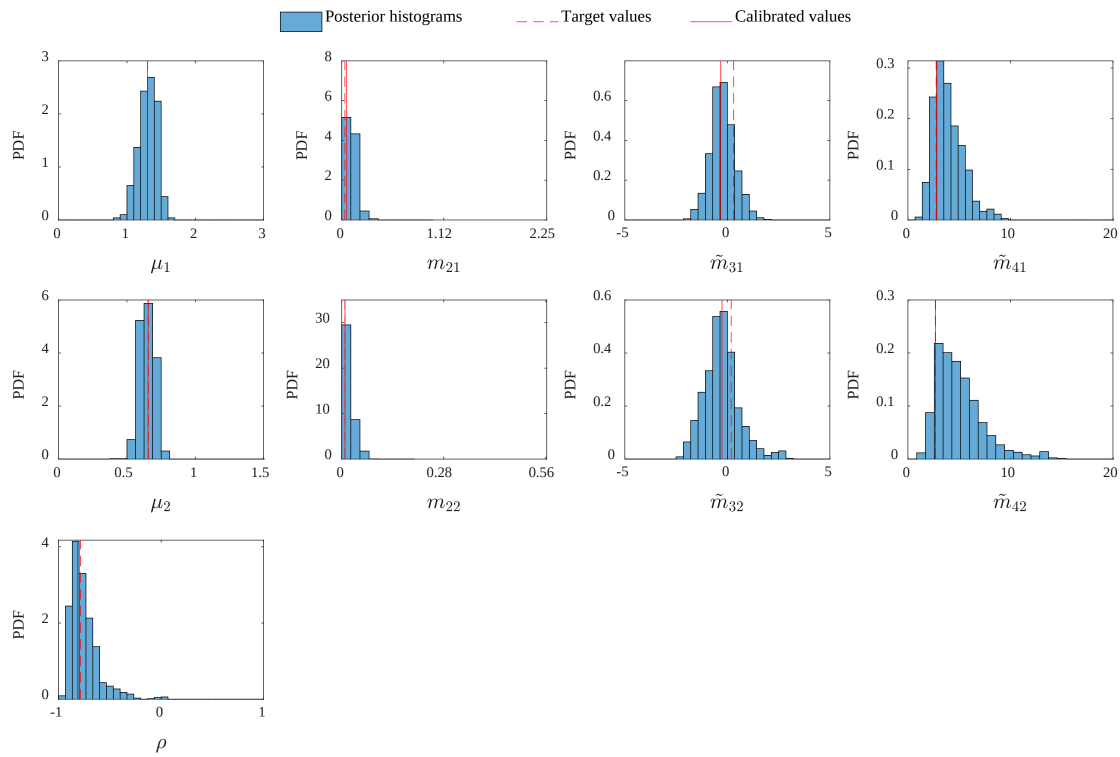

Fig. 4. Posterior PDFs of the inferred parameters.

Table 3. Calibrated parameters of the 2-DOF model.

Parameter	Target value	Calibrated value	Calibrated value without correlation
μ_1	1.3007	1.3000 (-0.05 %)	1.1214 (-13.78 %)
m_{21}	0.0348	0.0550 (48.85 %)	0.0157 (-54.89 %)
$\tilde{m}_{31}$	0.3102	-0.3200 (-203.16 %)	0.0022 (-99.29 %)
$\tilde{m}_{41}$	2.7503	2.8300 (2.90 %)	2.2912 (-16.69 %)
μ_2	0.6568	0.6540 (-0.43 %)	0.7474 (13.79 %)
m_{22}	0.0085	0.0090 (5.88 %)	0.0031 (63.53 %)
$\tilde{m}_{32}$	0.1866	-0.1780 (-195.39 %)	-0.0849 (-145.50 %)
$\tilde{m}_{42}$	2.6679	2.7000 (1.20 %)	2.4355 (-8.71 %)
ρ_{12}	-0.7858	-0.8172 (-4.00 %)	–

To further demonstrate the results, the sample sets of the input parameters $\boldsymbol{x}$ are generated from the calibrated joint distribution (i.e., the Gaussian copula function with the marginal staircase density functions) and are illustrated in Fig. 5. It can be seen that the samples generated from the calibrated distribution show good agreement with the target distribution. Meanwhile, the Bayesian updating of only the marginal staircase density functions is also performed to demonstrate how the stochastic model updating fails by ignoring the parameter dependency. The calibrated values of all the hyper-parameters are listed in the last column of Table 3. Most of the parameters denote quite large relative errors compared with those estimated with considering the parameter dependency. The sample sets of the input parameters $\boldsymbol{x}$ generated from the calibrated uncorrelated staircase density functions are also plotted in the figure, which are only distributed in a part of the target distribution, implying the importance of considering the parameter dependency in stochastic model updating.

Finally, Fig. 6 illustrates the updated simulated features of f_1 and f_2 that is obtained by assigning the calibrated joint distribution to $\boldsymbol{x}$, together with the initial simulated and target observed features. Moreover, the simulated features are also computed for the case ignoring the parameter dependency, and are provided in the figure. It can be seen that the updated simulated features show a distribution equivalent to the observed features for both cases with and without the parameter dependency, while the former provides better results. It implies that the Bhattacharyya distance metric has a potential to recreate wholly the distribution of the target observed features regardless of the consideration of the parameter dependency. Nonetheless, these results emphasize the importance of consideration of the parameter dependency in the stochastic model updating, because even though the observed features can be ideally quantified, the incompletely calibrated joint distribution of the input parameters could result in an inaccurate prediction of other quantity of interests, which might be important for the risk assessment or design optimization of the target structure.

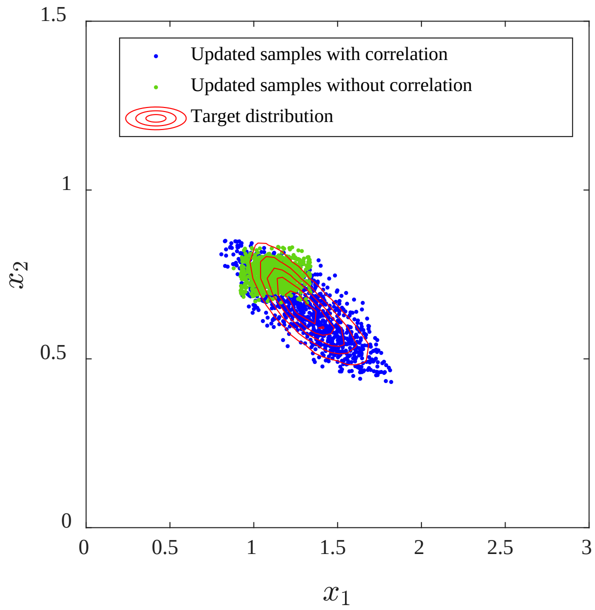

Fig. 5. Updated samples of the input parameters.

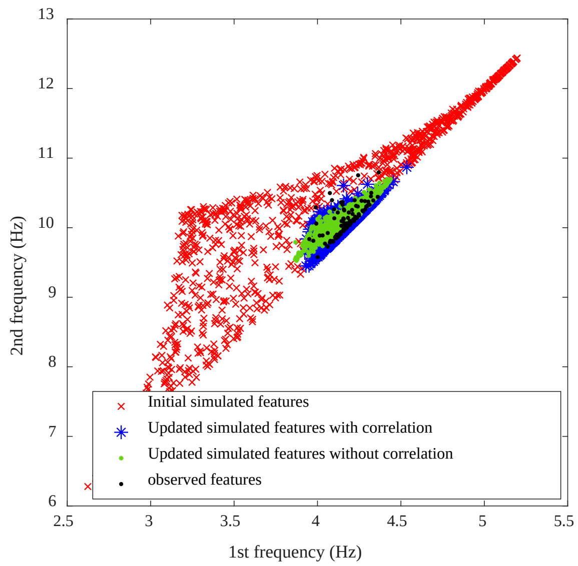

Fig. 6. Updated simulated features.

4.2. Case study II: The three degree of freedom spring-mass system

The next case study is performed on a 3-DOF spring-mass system illustrated in Fig. 7. This case study aims at demonstrating the capability of the proposed updating procedure for multivariate case. This numerical system has been employed for demonstrating various stochastic updating techniques [5,11], however, the uncertainty characteristics of the system are changed in this study to demonstrate the proposed approach. The stiffness coefficients k_1, k_2, and k_3 are considered as the uncertain input parameters to be calibrated, whereas the remaining parameters (i.e. k_4 to k_6 and the three masses m_1 to m_3) are treated to be the deterministic values: $k_{4-6} = 5.0$ N/m, $m_1 = 0.7$ kg, $m_2 = 0.5$ kg, and $m_3 =$

0.3 kg. The first three natural frequencies f_1, f_2, and f_3 are employed as the target output features the uncertainty characteristics of which are driven by the joint probabilistic distribution of k_1, k_2, and k_3 that is assumed to be a correlated tri-variate Gaussian distribution. The given support domains of k_1, k_2, and k_3 and the target values of both the hyper-parameters and correlation coefficients are shown in Table 4. It is noted that the support domains are set to cover more than 99.99 % confidence intervals of the target marginal distributions. Such notification is important because the support domain of the target joint distribution is not bounded, differently from the initial case study.

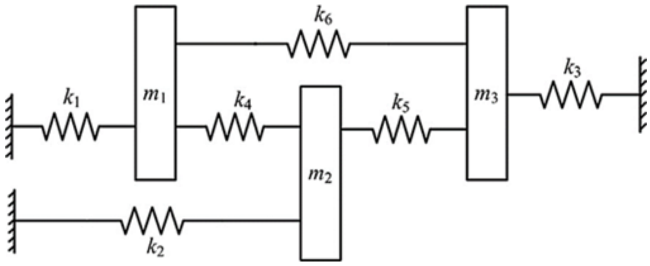

Fig. 7. 3-DOF spring-mass system.

Table 4. Uncertainty characteristics of the 3-DOF system.

Parameter	Support domain	Target distribution
k_1, k_2, k_3	$k_1 \in [2.5, 5.5]$, $k_2 \in [4.5, 5.5]$, $k_3 \in [5, 7]$	Gaussian, $\mu_1 = 4.0$, $\mu_2 = 5.0$, $\mu_3 = 6.0$, $m_{21} = 0.09$, $m_{22} = 0.01$, $m_{23} = 0.04$, $\rho_{12} = 0$, $\rho_{13} = -0.6$, $\rho_{23} = 0.6$
k_4–k_6, m_1–m_3	Deterministic	–

Consider the number of observed features be $N_{\text{obs}} = 500$, N_{obs} sample sets of k_1, k_2, and k_3 are generated from the target joint distribution and then the corresponding observed features $\mathbf{Y}_{\text{obs}}$, which comprise f_1, f_2, and f_3, are collected by evaluating the model with these sample sets.

On the other hand, let the sample size be $N_{\text{MC}} = 1000$, N_{MC} sets of the initial values of the hyper-parameters $\boldsymbol{\theta}_{k_1}$, $\boldsymbol{\theta}_{k_2}$, and $\boldsymbol{\theta}_{k_3}$ and the correlation coefficients ρ_{12}, ρ_{13}, and ρ_{23}, satisfying the moment constraints Θ_1, Θ_2, and Θ_3 and the correlation coefficient constraint $\mathcal{P}$, are generated by the rejection sampling in the support domains. For each set of the hyper-parameters and correlation coefficients, the joint distribution of the three stiffness parameters described by the Gaussian copula function with the marginal staircase density functions is determined. The number of bins n_b is set as the same value as that in the first case study. The number of simulated features is set to be $N_{\text{sim}} = 1000$, so that totally N_{sim} sample sets of k_1, k_2, and k_3 are generated from each joint distribution. Then, the corresponding initial simulated features are collected by evaluating the model for each sample sets. Fig. 8 compares the histograms and scatters between the observed features and arbitrary chosen simulated features.

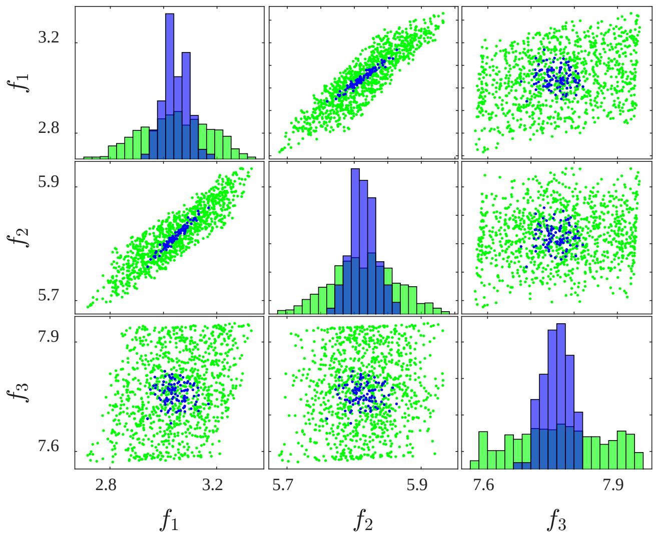

Fig. 8. Observed features in blue and initial simulated features in green, with the unit in Hz.

The Bhattacharyya distance is estimated for each set of the initial simulated features. The number of bins n_{bin} is chosen as the same value as that in the first case study. Then, the Bayesian updating of in total 15 inferred parameters, i.e., $\boldsymbol{\theta}_{k_i} = \{\mu_i, m_{2i}, \widetilde{m}_{3i}, \widetilde{m}_{4i}\}$, for $i = 1, 2, 3$, and ρ_{ij}, for $i = 1, 2$ and $j = i + 1, 3$, is performed using the Bhattacharyya distance-based likelihood function. The width factor ε is set to be $\varepsilon = 0.01$.

By employing in total 17 TMCMC iterations, all the inferred parameters are well updated to the posterior PDFs. The calibrated values (i.e., the MPVs of the posterior PDFs) of all inferred parameters are presented in Table 5, together with the corresponding target values. The relative estimation errors are also provided in the parentheses after the calibrated values. Note that the errors are not provided for the skewnesses and the correlation coefficient ρ_{12} because their true values are zero. It can be seen that the calibrated values of the mean and variance parameters are in good agreement with the target values with the largest relative error less than 5 %. On the contrary, the skewness parameters exhibit differences compared with the target values, especially for $\widetilde{m}_{31}$. However, these calibrated values are small enough for resulting in almost symmetric distributions as similar as the target distributions as depicted in Fig. 9. The kurtosis parameters also exhibit large errors compared with their target values, whereas these errors are also permissible to obtain reasonable distributions compared with the target distributions as illustrated in Fig. 9. As such, both the skewness and kurtosis parameters are relatively insensitive to the uncertainty characteristics of the target output features, compared with the means and variances. It is noted that, it does not mean that such higher order moment parameters are always insensitive to the target output features. In fact, in the previous example, the kurtosis parameters are precisely updated, implying that they are sensitive to the target output features in that example. More importantly, all correlation coefficients are in good agreement with their target values with the largest relative error around 10 %, implying that the proposed procedure is capable to properly capture the correlation structure regardless of no, negative, and positive correlations.

Table 5. Calibrated parameters of the 3-DOF system.

Parameter	Target value	Calibrated value
μ_1	4.0	4.0286 (0.72 %)
m_{21}	0.09	0.0890 (-1.11 %)
$\widetilde{m}_{31}$	0	0.2220
$\widetilde{m}_{41}$	3.0	4.4400 (48.00 %)
μ_2	5.0	5.0035 (0.07 %)
m_{22}	0.01	0.0104 (4.00 %)
$\widetilde{m}_{32}$	0	-0.0500
$\widetilde{m}_{42}$	3.0	3.8100 (27.00 %)
μ_3	6.0	6.0030 (0.05 %)
m_{23}	0.04	0.0410 (2.50 %)
$\widetilde{m}_{33}$	0	-0.0214
$\widetilde{m}_{43}$	3.0	3.9400 (31.33 %)
ρ_{12}	0	-0.0058
ρ_{13}	-0.6	-0.5728 (4.53 %)
ρ_{23}	0.6	0.5398 (10.03 %)

The joint distribution of k_1, k_2, and k_3 is then obtained as the Gaussian copula function having the marginal staircase density functions, assigned the calibrated values of the hyper-parameters and correlation coefficients. Fig. 9 shows the marginal CDF of each stiffness, along with the corresponding target marginal distribution. It is noted that, since the marginal distributions are obtained as staircase (i.e., discrete) density functions, the CDFs are estimated from the samples generated according to the staircase density functions, via the kernel density estimation. As can be seen, the estimated staircase density functions are in good agreement with their target marginal distribution, which supports that the aforementioned estimate errors in the skewness and kurtosis parameters are still permissible for calibrating the joint distribution of the parameters. Nevertheless, it is noted that, in the tail regions, the calibrated distributions, in particular for k_1, remain discrepancy from the target distributions due to the estimate errors in the kurtosis parameters, while the discrepancy in the tail regions do not affect greatly the model outputs as depicted in Fig. 10. Moreover, the obtained distributions have bounded support domains which are identical to ranges of the horizontal axes of Fig. 9 because of the definition of the staircase density functions, whereas the target Gaussian distributions do not have the bounded supports. It implies that the proposed procedure does not limit its applicability to the case where the investigated parameters have bounded supports, however, at the same time, it also indicates that the calibrated joint distribution cannot be employed for reliability analysis, where the target is estimating the probabilities of rare events that can be occurred out of the support domains. It is noted that, this limitation does not prevent the use of the proposed procedure in the stochastic model updating, since the main motivation of the stochastic model updating is to obtain the model that is capable to describe the system of interest conditioned on the observed data whereas reliability analysis is only one of the potential usages of the calibrated model.

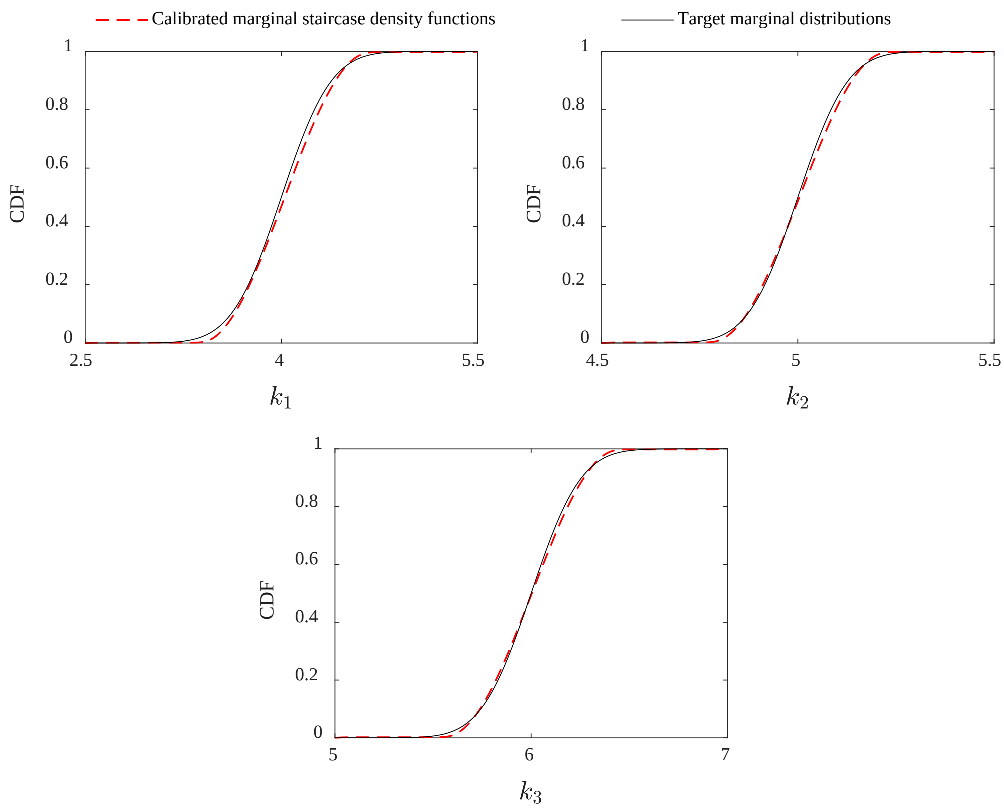

Fig. 9. Calibrated marginal distributions of the input parameters.

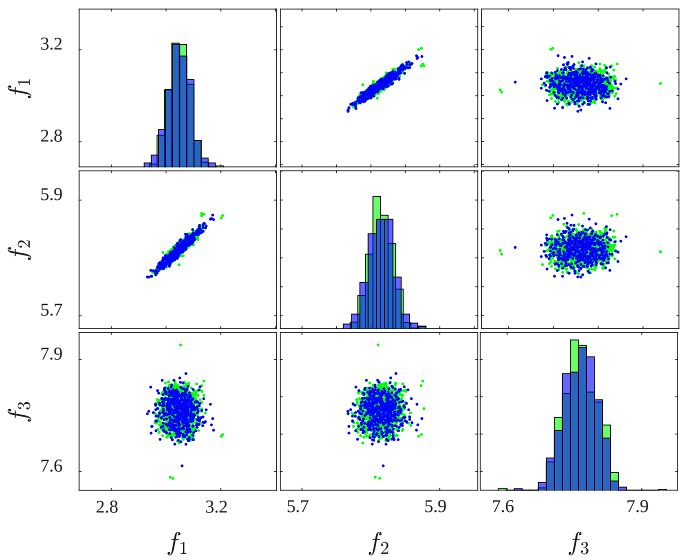

Fig. 10. Observed features in blue and updated simulated features in green, with the unit in Hz.

Finally, Fig. 10 compares the histograms and scatters between the target and updated simulated features. Compared with the initial simulated features in Fig. 8, It can be seen that the uncertainties in the three stiffness parameters are correctly calibrated by the proposed procedure and the calibrated model is capable to recreate wholly the uncertainty characteristics of the observed features. As such, the relatively large errors in the higher order moment parameters can be considered to be permissible, since the proposed procedure aims at not estimating the individual moment parameters precisely but rather obtaining model outputs which are identical to the observations to which some higher moment parameters might be relatively insensitive.

5. Nonlinear dynamic system updating

5.1. Problem description

The proposed approach is further demonstrated on the updating of nonlinear dynamic systems using the measured time signals. For this purpose, a model updating problem of a reinforced concrete (RC) bridge pier using simulated seismic response data is investigated. The target bridge is a seismic-isolated bridge with lead rubber bearings, designed based on the specifications for highway bridges in Japan [36]. Its structural descriptions are detailed in Table 6. Fig. 11 shows the 2-DOF lumped mass model as the numerical model of the target structure, in which the two lumped masses represent the superstructure and RC pier, and the two horizontal springs denote the rubber bearings and RC pier. The boundary condition at the surface is assumed to be fixed. The nonlinearity of the rubber bearings is characterized by a bilinear model with the ratio of the yield stiffness K_{B1} to the post-yield stiffness K_{B2} of 6.5:1 based on the manual on bearings for highway bridges in Japan [37]. Meanwhile, that of the RC pier is characterized by a bilinear model with the elastoplastic characteristic and the stiffness degradation model, namely Takeda model [38]. The well-known Rayleigh damping model is utilized as the damping model in which the damping ratios of the rubber bearings and RC pier are set to be 0 % and 2 %, respectively.

Table 6. Descriptions of the target bridge pier.

	Structural parameter	Nominal value
Superstructure	Mass M_S (ton)	604.0
Rubber bearings	Yield strength (kN)	1118
	Yield stiffness K_{B1} (kN/m)	40000
	Post-yield stiffness K_{B2} (kN/m)	6000
RC pier	Mass M_P (ton)	346.2
	Yield strength (kN)	3374
	Yield stiffness K_P (kN/m)	110100
	Yield displacement (m)	0.0306

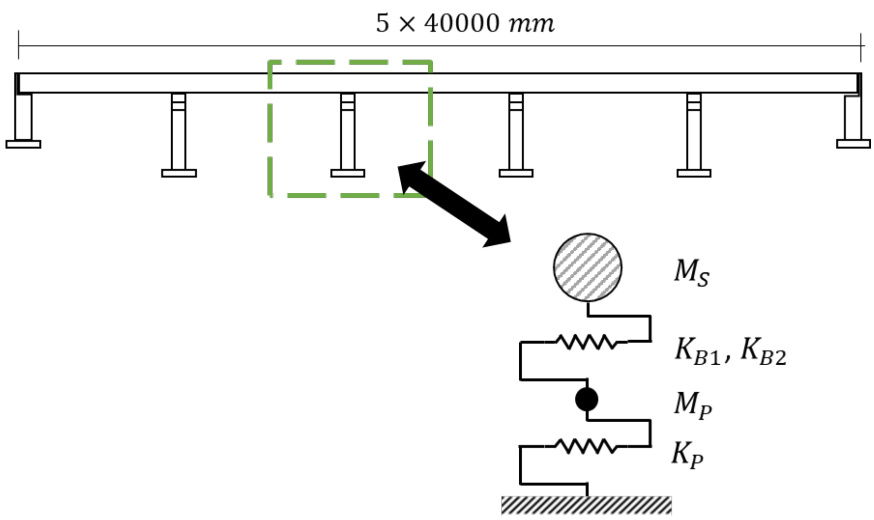

Fig. 11. Numerical modeling of the target bridge pier.

The aim of this updating problem is to quantify the uncertainty characteristics of the post-yield stiffness of the rubber bearings, K_{B2}, which governs the nonlinear behaviour of the target bridge pier under strong earthquakes, as well as the remaining stiffnesses K_{B1} and K_P. These three stiffnesses are parameterized as $K_{B1} = \bar{K}_{B1}x_1$, $K_{B2} = \bar{K}_{B2}x_2$, and $K_P = \bar{K}_P x_3$, where $\boldsymbol{x} = [x_1, x_2, x_3]$ are uncertain input parameters, and $\bar{K}_{B1}$, $\bar{K}_{B2}$, and $\bar{K}_P$ are the nominal values shown in Table 6. The other parameters are assumed to be fixed constants with the nominal values. The time-history of the acceleration response at the superstructure subjected to the level-2 type-II-II-1 earthquake introduced in Ref. [36] is used as the target output features. The duration time of the input ground motion is 40 s. Time history analysis of the 2- DOF model is performed using the Newmark β method ($\beta = 1/4$ and $\gamma = 1/2$) with the time step $\Delta t = 0.001$ s. Fig. 12 illustrates the time-history of the acceleration response at the superstructure and the force-displacement responses of the rubber bearings and pier for the case when all parameters are fixed to the nominal values shown in Table 6.

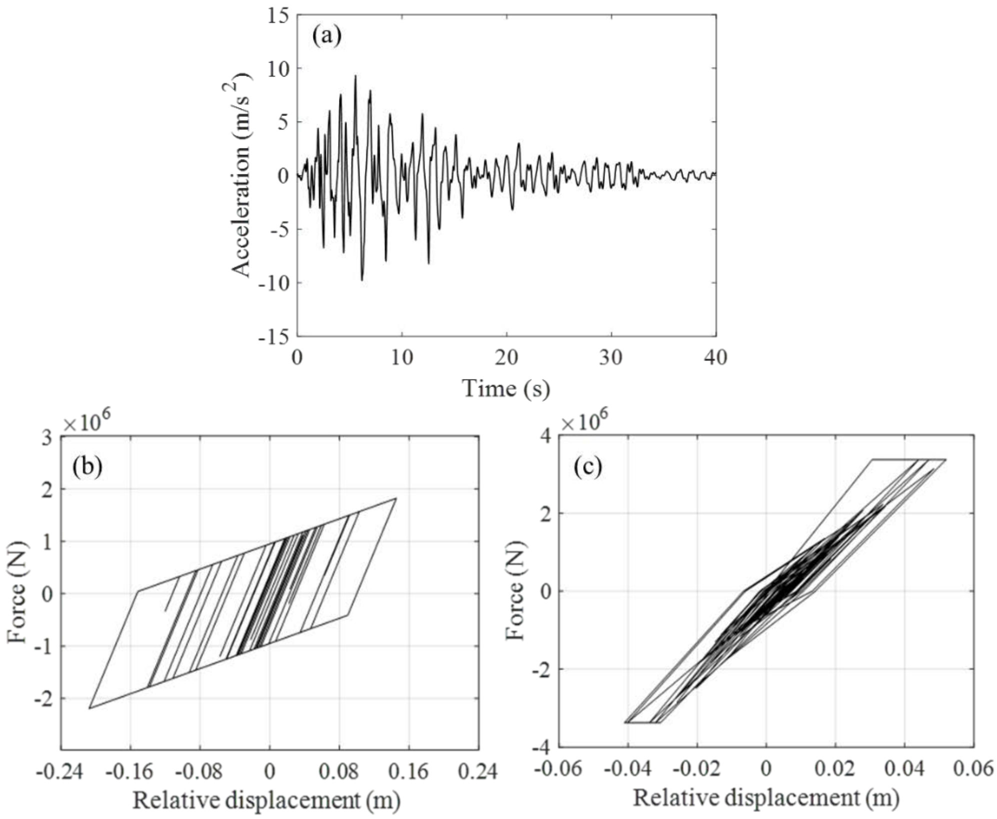

Fig. 12. (a) Time-history of the acceleration response at superstructure; (b) Force-displacement response of rubber bearings; (c) Force-displacement response of RC pier.

The target joint distribution of the input parameters $\boldsymbol{x}$ is considered to be a correlated tri-variate Gaussian distribution, in which a positive correlation between x_1 and x_2 (i.e., between the initial and post stiffnesses of the rubber bearings) is introduced. The pre-defined support domains of x_1, x_2, and x_3 and the target values of the hyper-parameters and correlation coefficients are detailed in Table 7. Similar to the previous case study, the support domains are determined to cover more than 99.99 % confidence intervals of their target marginal distributions. Suppose the number of observed features be $N_{\text{obs}} = 100$, N_{obs} sample sets of the input parameters $\boldsymbol{x}$ are generated according to the target joint distribution and then the corresponding observed features $\mathbf{Y}_{\text{obs}}$ of the time-history of the acceleration response at the superstructure, are collected by evaluating the model with these sample sets.

Table 7. Uncertainty characteristics of the target bridge pier.

Parameter	Support set	Target distribution
x_1, x_2, x_3	$x_1 \in [0.7, 1.3]$, $x_2 \in [0.7, 1.3]$, $x_3 \in [0.7, 1.3]$	Gaussian, $\mu_1 = 1.0$, $\mu_2 = 1.0$, $\mu_3 = 1.0$, $m_{21} = 0.0049$, $m_{22} = 0.0049$, $m_{23} = 0.0049$, $\rho_{12} = 0.8$, $\rho_{13} = 0$, $\rho_{23} = 0$
M_S, M_P	Deterministic	–

In this example, totally 13 inferred parameters, i.e., the hyper-parameters $\boldsymbol{\theta}_{x_i} = \{\mu_i, m_{2i}, m_{3i}, m_{4i}\}$, for $i = 1, 2, 3$, and correlation coefficient ρ_{12} is taken into account. Note that the remaining correlation coefficients are assumed to be zero in advance and ignored in the updating procedure. Suppose the sample size be $N_{\mathrm{MC}} = 100$, N_{MC} sets of the hyper-parameters maintaining the moment constraints Θ_1 Θ_2, and Θ_3, are generated by the rejection sampling whereas N_{MC} sets of the correlation coefficient are arbitrary generated from the support of [-1, 1]. For each set of $[\boldsymbol{\theta}_{x_1}, \boldsymbol{\theta}_{x_2}, \boldsymbol{\theta}_{x_3}, \rho_{12}]$, the joint probability distribution of the input parameters $\boldsymbol{x}$ is defined as the Gaussian copula function having the marginal staircase density functions. The number of bins n_b is chosen to be $n_b = 50$. The number of simulated features, on the other hand, is set as $N_{\mathrm{sim}} = 500$; hence, N_{sim} sample sets of $\boldsymbol{x}$ are generated from each joint distribution $\left\{F_{\mathbf{x}}^{(k)}: k = 1, \cdots, N_{\mathrm{MC}}\right\}$, and then the corresponding initial simulated features $\mathbf{Y}_{\mathrm{sim}}^{(k)}$ are obtained by evaluating the model with these samples. The window length in the dimension reduction procedure introduced in Section 2.1 is set to be $\mathrm{L} = 0.025(t+1)$, with $t = 40/0.001 = 40000$. Hence, the RMS matrices of both the simulated and observed features, $\mathbf{R}^s_{\mathbf{Y}_{\mathrm{sim}}^{(k)}}$ and $\mathbf{R}^s_{\mathbf{Y}_{\mathrm{sim}}}$, for $\forall s = 1, \cdots, 40$, are defined. Fig. 13 compares the histograms and scatters between the observed and simulated features by employing five arbitrary selected RMS matrices of $s = 30, 7, 6, 9, 37$. The figure demonstrates that the target features show strong nonlinearity, making the updating problem significantly challenging. The Bhattacharyya distance is estimated for each pair of the simulated and observed RMS matrices, and the RMS value of the Bhattacharyya distances, R_{d_B}, is used as the UQ metric in the approximate likelihood. The number of bins n_{bin} is chosen as $n_{\mathrm{bin}} = 10$ while the width factor ε is set as $\varepsilon = 0.01$.

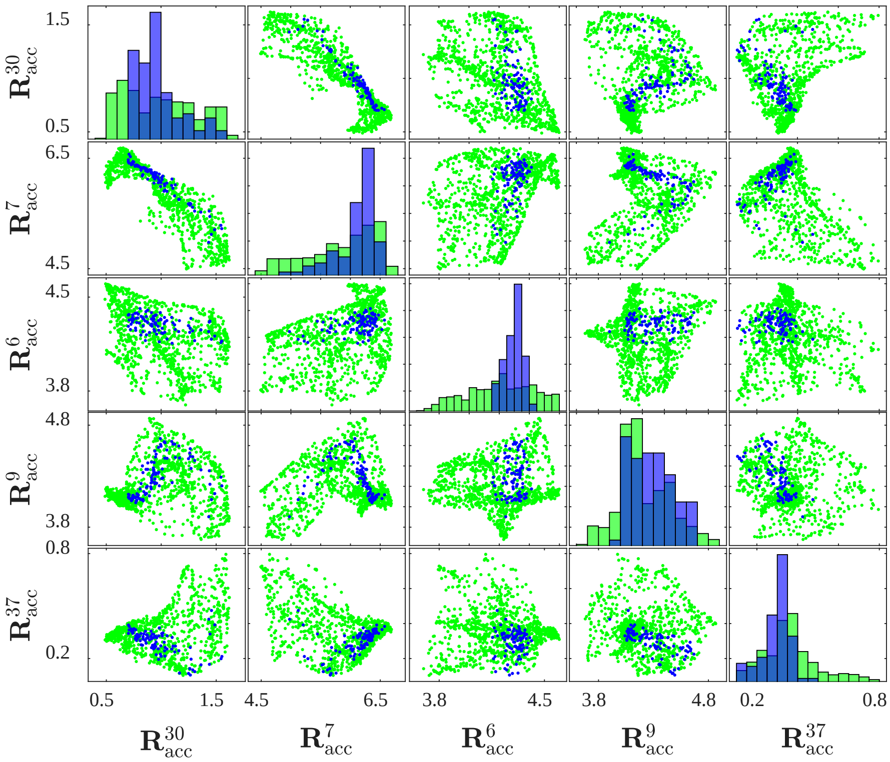

Fig. 13. Observed features in blue and initial simulated features in green, with the unit in $\mathrm{m/s^2}$.

5.2. Results assessment

By employing totally 13 TMCMC iterations, all the inferred parameters are well updated to the posterior PDFs. The calibrated values of the inferred parameters are detailed in Table 8, together with the corresponding target values. The relative estimation errors are also shown in the parentheses after the calibrated values. The calibrated values of all mean parameters and the variance parameter m_{21} are in good agreement with the target values, while the remaining variance parameters exhibit large estimate errors due to their quite small target values. In spite of the large relative errors, the calibrated values of the variance parameters are close to the target values compared with the prior supports and these errors are permissible to result in the model outputs close to the observations. In addition, the skewnesses and kurtoses exhibit differences compared with their target values, while these errors are also within allowable limits to achieve the model outputs close to the target observations, as similar as the previous example. Moreover, the positive correlation induced is also captured by the proposed procedure though a certain error is still remained compared with the target value. By assigning these calibrated values, the joint distribution of $\boldsymbol{x}$ is tuned identical to the target distribution.

Table 8. Calibrated parameters of the target bridge pier model.

Parameter	Target value	Calibrated value
μ_1	1.0	0.9958 (-0.42 %)
m_{21}	0.0049	0.0045 (-4.44 %)
$\tilde{m}_{31}$	0	-0.1688
$\tilde{m}_{41}$	3.0	4.3450 (44.83 %)
μ_2	1.0	0.9992 (-0.08 %)
m_{22}	0.0049	0.0065 (32.65 %)
$\tilde{m}_{32}$	0	0.4050
$\tilde{m}_{42}$	3.0	3.9500 (31.67 %)
μ_3	1.0	0.9996 (-0.04 %)
m_{23}	0.0049	0.0068 (38.78 %)
$\tilde{m}_{33}$	0	-0.3025
$\tilde{m}_{43}$	3.0	4.3960 (46.53 %)
ρ_{12}	0.8	0.6736 (-15.80 %)

Finally, Fig. 14 compares the histograms and scatters between the target and simulated features for the five arbitrary selected RMS matrices of $s = 30, 7, 6, 9, 37$. Compared with the initial simulated features in Fig. 13, It can be seen the updated simulated features are identical to the observed features capturing the complicated nonlinear structure. This indicates the feasibility of the proposed approach in the stochastic model updating of nonlinear dynamic systems for recreating wholly the uncertainty characteristics of the target measured time signals, even though the prior knowledge about the joint distribution of the parameters is extremely limited.

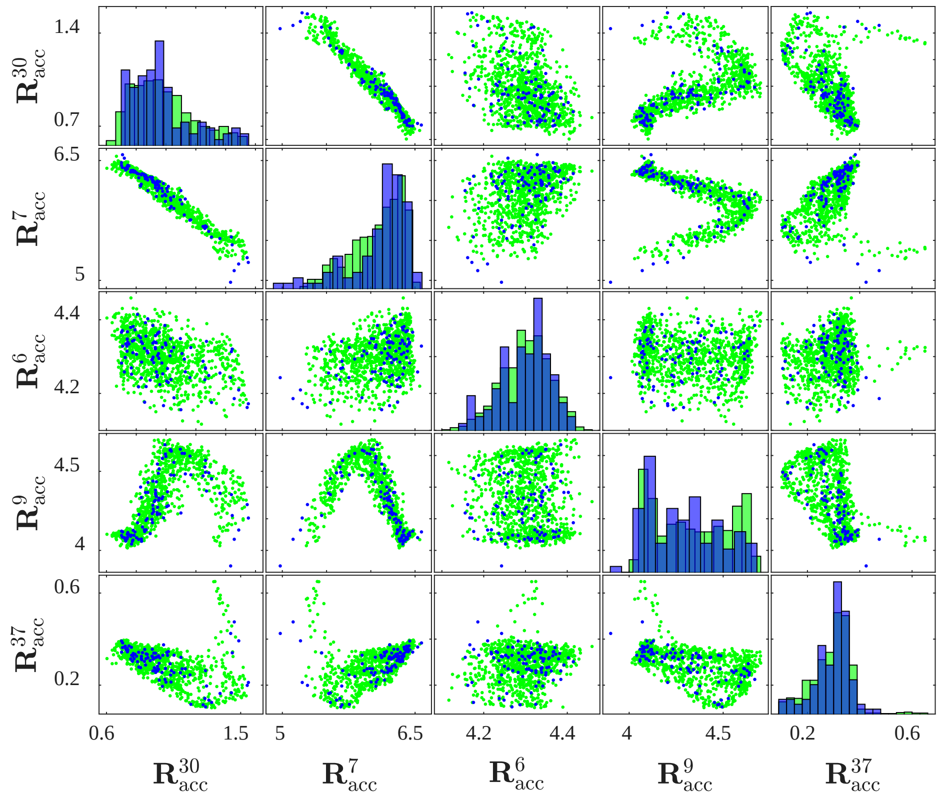

Fig. 14. Observed features in blue and updated simulated features in green, with the unit in m/s^2.

6. Conclusions

This paper presents three contributions for calibrating the joint probabilistic distribution of the correlated parameters through the stochastic model updating by a limited number of measurement data. First, each marginal distribution is characterized by staircase density functions and their hyper-parameters are subjected to be updated. The staircase density functions can flexibly describe a broad range of distributions; thus, no limiting hypotheses on the distribution families is required differently from the most of the stochastic model updating methods. Next, the dependence structure among the parameters are described by the Gaussian copula. The correlation coefficients are also subjected to be updated; thus, even the prior knowledge on the presence of parameter dependencies is not required. Finally, the Bhattacharyya distance-based UQ metric is proposed to define an approximate likelihood capable of quantifying the stochastic discrepancy between the model outputs and measurements. As such, the inferred parameters, i.e., the hyper-parameters and correlation coefficients are successfully updated through the Bayesian model updating. Two exemplary applications and followed nonlinear dynamic system updating problem demonstrate the feasibility of the proposed updating framework and the importance of considering the parameter dependency in the stochastic model updating.

However, open problems still exist. First, the cost function in the optimization problem solved for estimating the staircase density function is solely selected in this study. The staircase density that attains other optimality criteria, such as the maximal entropy, can be similarly formulated, but further studies are necessary to investigate the most suitable choice of the cost function for model updating. Second, the Gaussian copula might not be suitable if the parameters demonstrate a strong nonlinear dependency. The assumption on the copula function type introduces another source of uncertainty, i.e., the model bias, and such uncertainty should be quantified by, for instance, the Bayesian model class selection. These two challenges will be addressed in the future work.

Declaration of competing interest

The authors declare that they have no known competing financial interests or personal relationships that could have appeared to influence the work reported in this paper.

Acknowledgments

The first author acknowledges the support of the Deutsche Forschungsgemensschaft (DFG, German Research Foundation) — SFB1463-434502799.

References

1. J.E. Mottershead, M, Ling, M.I. Friswell, The sensitivity method in finite element model updating: A tutorial, Mech. Syst. Signal Process. 25 (2011) 2275-2296.
2. E. Patelli, Y, Govers, M. Broggi, H.M. Gomes, M. Ling, J.E. Mottershead, Sensitivity or Bayesian model updating: a comparison of techniques using the DLR AIRMOD test data. Arch. Appl. Mech. 87 (2017) 905-925.
3. J.E. Mottershead, M.I. Friswell, Model Updating In Structural Dynamics. J. Sound Vib. 167 (1993) 347-375.
4. D. Shan, Q. Li, I. Khan, X. Zhou, A novel finite element model updating method based on substructure and response surface model, Eng. Struct. 103 (2015) 147-156.
5. C. Mares, J.E. Mottershead, M.I. Friswell, Stochastic model updating: Part 1—theory and simulated example, Mech. Syst. Signal Process. 20 (2006) 1674-1695.
6. H.H. Khodaparast, J.E. Mottershead, M.I. Friswell, Perturbation methods for the estimation of parameter variability in stochastic model updating, Mech. Syst. Signal Process. 22 (2008) 1751-1773.

7. K.K. Sairajan, G.S. Aglietti, Robustness of system equivalent reduction expansion process on spacecraft structure model validation, AIAA J. 50 (2012) 2376-2388.
8. S. Bi, S. Prabhu, S. Cogan, S. Atamturktur, Uncertainty quantification metrics with varying statistical information in model calibration and validation, AIAA J. 55 (2017) 3570-3583.
9. B. Goller, M. Broggi, A. Calvi, G.I. Schuëller, A stochastic model updating technique for complex aerospace structures, Finite Elem. Anal. Des. 47 (2011) 739-752.
10. Y. Govers, M. Link, Stochastic model updating—Covariance matrix adjustment from uncertain experimental modal data, Mech. Syst. Signal Process. 24 (2010) 696-706.
11. S. Bi, M. Broggi, M. Beer, The role of the Bhattacharyya distance in stochastic model updating, Mech. Syst. Signal Process. 117 (2019) 437-452.
12. M.A. Beaumont, W. Zhang, D.J. Balding, Approximate Bayesian computation in population genetics, Genetics 162 (2002) 2025-2035.
13. B.M. Turner, T. Van Zandt, A tutorial on approximate Bayesian computation, J. Math. Psychol. 56 (2012) 69-85.
14. M. Kitahara, S. Bi, M. Broggi, M. Beer, Bayesian model updating in time domain with metamodel-based reliability method, J. Risk Uncertainty Eng. Syst. Part A: Civ. Eng. 7 (2021) 04021030.
15. L.G. Crespo, S.P. Kenny, The NASA Langley multidisciplinary uncertainty quantification challenge, Mech. Syst. Signal Process. 152 (2021) 107405.
16. M. Kitahara, S. Bi, M. Broggi, M. Beer, Nonparametric Bayesian stochastic model updating with hybrid uncertainties, Mech. Syst. Signal Process. 163 (2022) 108195.
17. L.G. Crespo, S.P. Kenny, D.P. Giesy, B.K. Stanford, Random variables with moment-matching staircase density function, Appl. Math. Model 64 (2018) 196-213.
18. X.S Tang, D.Q. Li, C.B. Zhou, K.K. Phoon, L.M. Zhang, Impact of copulas for modeling bivariate distributions on system reliability, Struct. Safety 44 (2013) 80-90.
19. D.Q. Li, L. Zhang, X.S. Tang, W. Zhou, J.H. Li, C.B. Zhou, K.K. Phoon, Bivariate distribution of shear strength parameters using copulas and its impact on geotechnical system reliability, Compt. Geotech. 68 (2015) 184-195.
20. X.S Tang, D.Q. Li, C.B. Zhou, K.K. Phoon, Copula-based approaches for evaluatig slope reliability under incomplete probability information, Struct. Safety 52 (2015) 90-99.
21. A. Bhattacharyya, On a measure of divergence between two multinominal populations, Indian J. Stat. 7 (1964) 401-406.
22. B.K. Patra, R. Launonen, V. Ollikainen, S. Nandi, A new similarity measure using Bhattacharyya coefficient for collaborative filtering in sparse data, Knowledge-Based Syst. 82 (2015) 163-177.
23. R. Sharma, S. Devi, G. Kapoor, N.S. Barnett, A brief note on some bounds connecting lower order moments for random variables defined on a finite interval, Int. J. Theor. Appl. Sci. 1 (2009) 83-85.
24. P. Kumar, Moment inequalities of a random variable defined over a finite interval, J. Inequ. Pure. Appl. Math. 3 (2002) 1-11.
25. R.B. Nelsen, An Introduction to Copulas; 2nd ed, Springer, New York, 2006.
26. L.H. Haff, Parameter estimation for pair-copula constructions, Bernoulli 19 (2013) 462-491.

27. J.L. Beck, L.S. Katafygiotis, Updating models and their uncertainties. I: Bayesian statistical framework, J. Eng. Mech. 124 (1998) 455-461.
28. J.L. Beck, S.K. Au, Bayesian updating of structural models and reliability using Markov chain Monte Carlo simulation, J. Eng. Mech. 128 (2002) 380-391.
29. J. Ching, Y.C. Chen, Transitional Markov chain Monte Carlo method for Bayesian updating, model class selection, and model averaging, J. Eng. Mech. 133 (2007) 816-832.
30. W. Betz, I. Papaioannou, D. Straub, Transitional Markov chain Monte Carlo: Observations and improvements, J. Eng. Mech. 142 (2016).
31. E. Patelli, D.A. Alvarez, M. Broggi, M. de Angelis, Uncertanty management in multidisciplinary design of critical safety systems, J. Aerosp. Inf. Syst. 12 (2015) 140-169.
32. C. Safta, K. Sargsyan, H.N. Najm, K. Chowdhary, B. Debusschere, L.P. Swiler, M.S. Eldred, Probabilistic methods for sensitivity analysis and calibration in the NASA challenge problem, J. Aerosp. Inf. Syst. 12 (2015) 219-234.
33. R. Rocchetta, M. Broggi, Q. Huchet, E. Patelli, On-line Bayesian model updating for structural health monitoring, Mech. Syst. Signal Process. 103 (2018) 174-195.
34. P. Li, Z. Lu, Y. Zhao, Bayesian updating of time-dependent structural reliability using the method of moment, J. Risk Uncertainty Eng. Syst. Part A: Civ. Eng. 7 (2021) 04021066.
35. B. Liao, R. Zhao, K. Yu, C. Liu, Stochastic model updating method for estimates of arbitrary distributed parameters using resampling technique, Appl. Math. Model. 105 (2022) 387-405.
36. Japan Road Association, Design specifications of highway bridges V: Seismic design, Maruzen, Tokyo, 2016.
37. Japan Road Association, Manual on bearings for highway bridges, Maruzen, Tokyo, 2004. (In Japanese).
38. T. Takeda, M.A. Sozen, N.N. Nielsen, Reinforced concrete response to simulated earthquakes, J. Struct. Div. 96 (1970) 2257-2573.